Analyst

Accepted Manuscript

This is an *Accepted Manuscript*, which has been through the Royal Society of Chemistry peer review process and has been accepted for publication.

Accepted Manuscripts are published online shortly after acceptance, before technical editing, formatting and proof reading. Using this free service, authors can make their results available to the community, in citable form, before we publish the edited article. We will replace this *Accepted Manuscript* with the edited and formatted *Advance Article* as soon as it is available.

You can find more information about *Accepted Manuscripts* in the Information for Authors.

Please note that technical editing may introduce minor changes to the text and/or graphics, which may alter content. The journal's standard Terms & Conditions and the Ethical guidelines still apply. In no event shall the Royal Society of Chemistry be held responsible for any errors or omissions in this *Accepted Manuscript* or any consequences arising from the use of any information it contains.

ROYAL SOCIETY OF CHEMISTRY

www.rsc.org/analyst

TOC Entry:

Exploring lipid information characteristic of non-Hodgkin's lymphoma from tissue sections and fine-needle aspirates using DESI – mass spectrometry and multivariate statistics.

Analyst Accepted Manuscript

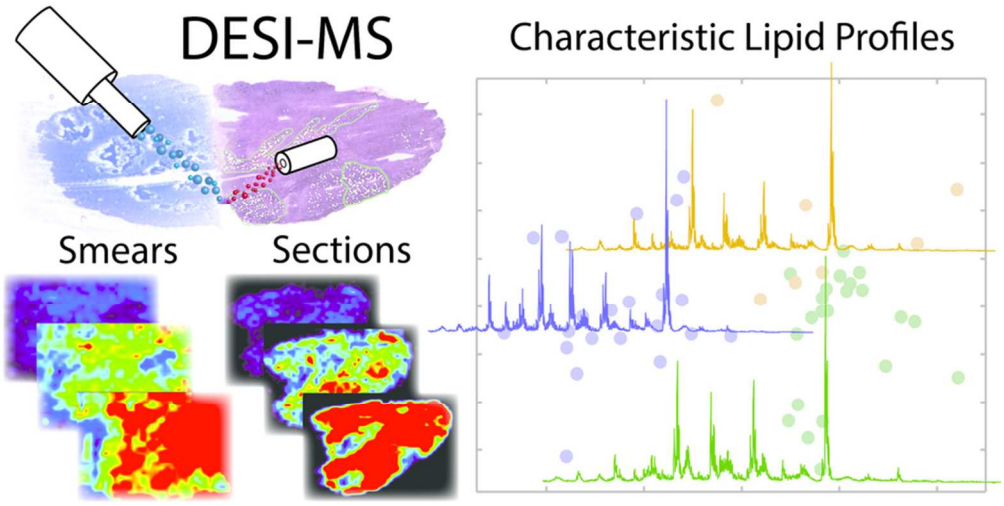

Graphical Abstract
40x20mm (600 x 600 DPI)

Analyst Accepted Manuscript

Please do not adjust margins

Journal Name

ARTICLE

Characteristic lipid profiles of canine non-Hodgkin's lymphoma from surgical biopsy tissue sections and fine needle aspirate smears by desorption electrospray ionization – mass spectrometry

Received 00th January 20xx,
Accepted 00th January 20xx

DOI: 10.1039/x0xx00000x

www.rsc.org/

Alan K. Jarmusch,[a, †] Kevin S. Kerian,[a, †] Valentina Pirro,[a] Tyler Peat,[b] Craig A. Thompson,[b] José A. Ramos-Vara,[b] Michael O. Childress,[c] and R. Graham Cooks[a]

Canine non-Hodgkin's lymphoma (NHL) is a heterogeneous group of cancers representing approximately 15% of all canine cancers. Further, canine NHL mimics human disease in regards to histopathology and clinical behavior and could function as a comparative model. Diagnosis is currently performed by histopathological evaluation of surgical biopsy specimens and fine needle aspirate (FNA) cytology, an alternative and less invasive method for diagnosis. Desorption electrospray ionization – mass spectrometry (DESI-MS) imaging was performed on tissue sections of surgical biopsies and FNA smears. Mass spectra acquired from normal lymph nodes and NHL tumors were explored using multivariate statistics (*e.g.* principal component analysis). Tissue sections yielded a predicted sensitivity of 100% for normal and 93.1% for tumor. Further, preliminary results suggest B-cell and T-cell lymphoma can be discriminated (CV sensitivity of 95.5% and 85.7%, respectively). Normal and B-cell NHL FNA samples analyzed by DESI produced spectra that were similar to spectra obtained from surgical biopsies. FNA samples were evaluated using a PCA-LDA classification system built using tissue section data, exploring if the chemical information obtained from the different sample types is similar and whether DESI-MS performed on FNA samples is of diagnostic value. FNA prediction rate for normal (85.7%) and B-cell NHL (89.3%) indicated that DESI-MS analysis of FNA, not previously explored, could provide rapid preliminary diagnosis. Certainly, MS provides complementary molecular information to be used in conjunction with histopathology/cytology, potentially improving diagnostic confidence. The methodology outlined here is applicable to canine NHL, further supports canine models of human NHL, and translation to humans is envisioned.

Introduction

Non-Hodgkin's lymphoma (NHL) is a diverse group of cancers, afflicting canines and humans. Rates of NHL in canines exceed that in humans;[1] nevertheless, NHL is the seventh most common human cancer in the United States resulting in an estimated 20,000 deaths in 2014.[2] NHL can be broadly defined into two subgroups, B-cell and T-cell, correlated to the lymphocyte immunophenotypes from which the cancer originated. B-cell lymphomas are the more common of the two, particularly diffuse large B-cell lymphoma, thus they are the primary focus of this study. Canine lymphoma is currently being considered as a meaningful comparative model for human NHL, while important in its own right.[1, 3] The gold standard for diagnosis of NHL is histopathological evaluation of surgically removed lymph node (whole or in part), which is commonly supported by immunohistochemical (IHC) analysis. Histopathological diagnosis is based on morphological and cytological features, such as morphological growth pattern, nuclear size and shape, and mitotic index.[4, 5] A less invasive alternative to surgical biopsy is fine needle aspirate (FNA) biopsy, performed using a hypodermic needle that is inserted into a suspicious lymph node. A small amount of cellular material is removed, expelled onto a microscope slide, and smeared to form a cellular monolayer which may be evaluated using light microscopy following cytochemical or immunocytochemical staining. FNA smears are suitable for screening and rapid preliminary diagnosis; however, smaller sample size and destruction of nodal architecture, a result of smearing, can result in higher rates of false negatives and inconclusive diagnoses.[6] FNA does have advantages over surgical biopsy and histopathology, in that it is less expensive, less invasive, and less technically demanding.[7, 8] Both canines and humans with NHL may be significantly debilitated at the time of initial cancer diagnosis, and a minimally invasive

[a] *Department of Chemistry and Center for Analytical Instrumentation Development, Purdue University, West Lafayette, IN 47907.*
[b] *Department of Comparative Pathobiology, College of Veterinary Medicine, Purdue University, West Lafayette, IN 47907*
[c] *Department of Veterinary Clinical Sciences, College of Veterinary Medicine, Purdue University, West Lafayette, IN 47907*
† Authors contributed equally to this work.
Electronic Supplementary Information (ESI) available: [details of any supplementary information available should be included here]. See DOI: 10.1039/x0xx00000x

Analyst Accepted Manuscript

Please do not adjust margins

diagnostic technique may be better suited to these patients than surgical biopsy. Therefore, identifying methods to enhance the quality of diagnostic information afforded by FNA smears would be worthwhile.

A promising method for improving the diagnostic yield of FNA biopsies is desorption electrospray ionization – mass spectrometry (DESI-MS), an ambient ionization technique which allows for chemical analysis of surfaces, including tissue, at native atmospheric conditions (temperature, pressure, and humidity). The mechanism of analyte desorption and ion generation has been extensively studied.[9, 10] Briefly, a stream of charged droplets impact the surface, create a thin film of solvent allowing analyte dissolution. Subsequent charged droplet impact sputters small analyte containing droplets which undergo evaporation and Coulombic fission generating ions via electrospray-like processes. DESI can be operated in an imaging mode, allowing chemical information to be mapped in two or more spatial dimensions.[11-16] DESI-MS imaging has been applied previously in canine bladder cancer[11] and human cancers, including those of the liver,[12] brain,[13] kidney,[20] prostate,[21] and other organs.[22] DESI-MS has been applied to human brain tissue smears obtained during surgery,[14] while differing from FNA smears in regards to collection and pathological evaluation. The analysis of lipids that compose cells, structurally and functionally, and tissue has been the focus of the previously mentioned studies, allowing for differentiation of cancer from normal tissue without exception. The lipid profile, *i.e.* type of lipid and quantity as reflected in the measured mass spectrum, varies with cell metabolism and signaling and is indicative of disease state. The use of multivariate statistics for pattern recognition, such as principal component analysis (PCA) followed by supervised classification techniques (*e.g.* linear discriminant analysis, LDA), allows for visualization and classification of differences between samples and complex relationships within large datasets.

In this paper we explore characteristic endogenous lipids using DESI-MS from surgical biopsy tissue sections and FNA smears for disease state differentiation (*i.e.* normal vs. tumor) in canine NHL. DESI-MS imaging of tissue sections detected lipid profiles indicative of disease state, which established a data set with which to compare FNA smears. Needle biopsies analyzed directly[24] or indirectly by ambient ionization - mass spectrometry have neither been demonstrated to be of diagnostic use nor shown to yield similar information to that of tissue section. The characteristic lipid profiles obtained from surgical biopsies and FNAs corroborate histopathology and cytology while providing unique chemical insight. Comparison between previous data regarding the significant lipids in human NHL and this canine study provide molecular support for a canine comparative model.

Methods

Specimens

Specimens were provided by the College of Veterinary Medicine, Purdue University. All NHL specimens were collected from pet dogs presented to the Purdue University Veterinary Teaching Hospital (PUVTH) for medical treatment of their cancer. At the time of presentation, fine needle aspirate samples were collected from an affected lymph node in each dog using a 22 gauge hypodermic needle. FNA samples were expelled onto glass slides, allowed to air dry, and then stored at -80°C until the time of DESI-MS analysis. Immediately following FNA, all dogs with NHL underwent surgical biopsy of the same affected peripheral lymph node. A portion of each biopsy was fixed in 10% neutral buffered formalin and submitted for histopathologic confirmation of NHL. The residual portion of each dog's lymph node biopsy was snap frozen in liquid nitrogen, and the samples were stored at -80°C until the time of DESI-MS analysis. Additional information pertaining to specimen 12, a metastatic carcinoma, can be found in the **Supplementary Material**. Lymph node samples from healthy, purpose-bred research dogs served as normal controls. All control animals had been humanely euthanatized as part of an academic laboratory course within the Purdue College of Veterinary Medicine Doctor of Veterinary Medicine degree curriculum. Surgical lymph node biopsy and FNA samples of peripheral lymph nodes were collected immediately post-mortem from all control animals in identical fashion to that described for pet dogs with NHL. All lymph nodes from control animals were confirmed to be histologically normal following light microscopic review of H&E stained sections from formalin-fixed tissues by a board-certified veterinary pathologist. All medical and surgical procedures conducted on both control animals and pet dogs were approved by the Purdue Animal Care and Use Committee (1111000308 and 1211000780).

DESI-MS analysis

Frozen surgical biopsy specimens were cryosectioned at 15µm thickness using a Cryotome FSE (Thermo, Waltham, MA, USA) and thaw mounted on glass microscope slides (Gold Seal Rite-On Microscope Slides, Thermo). Prior to analysis, the slides were allowed to come to room temperature and briefly dried using an electronic desiccator (VWR, Desi-Vac Container, Radnor, PA, USA) for approximately 10 minutes to remove any frozen condensation resulting from storage. FNA smears were also dried for ~10 minutes prior to analysis, for the same reason, and analyzed under the same conditions. Normal and tumor samples were randomized over multiple days of analysis, surgical biopsy tissue sections and specimen matched FNA were analyzed on the same day. DESI-MS was performed using a lab built prototype ionization source coupled to a linear ion trap mass spectrometer (LTQ, Thermo). DESI-MS was carried out in the negative ion mode using equal parts dimethylformamide (DMF) and acetonitrile (ACN), preserving tissue morphology and allowing subsequent histopathology to be performed on the analyzed tissue section.[25] DESI analysis was performed using the following major parameters: automatic gain control (AGC) off, maximum ion injection time

Analyst Accepted Manuscript

This journal is © The Royal Society of Chemistry 20xx

Please do not adjust margins

of 250 ms with 2 microscans, 5 kV spray voltage, 180 PSI N_2 (gas), incident spray angle was 52˚, capillary temperature of 275°C, spray-to-surface distance ~2 mm, and spray-to-MS inlet distance ~8 mm. Identical DESI-MS conditions were used to acquire high resolution mass spectrometry data on an orbitrap mass spectrometer (Exactive, Thermo). HRMS was interpreted using XCalibur and monoisotopic formulae masses were calculated in Isopro3. Sample slides were analyzed by securing them to the moving stage. The MS scan rate was coordinated with the moving stage speed in the "x" dimension (*i.e.* rows), defining resolution (200 µm). Upon the completion of each row, the moving stage was stepped vertically in 200 µm increments defining the "y" resolution. The typical time required for DESI imaging of a tissue section was less than 20 minutes. Illustrative is specimen 42, ~20 min, with an imaging area approximately 8.4 mm (width) by 7.6 mm (height), including the entirety of the tissue section roughly 6.2 mm (width) by 5.8 mm (height) in dimension.

Pathology

Histopathologic review, with tumor subtyping according to World Health Organization criteria,[4] was performed on formalin-fixed lymph node tissue sections as part of routine clinical diagnosis, see **Supplemental Table 1**. The clinical diagnosis was used for DESI-MS data correlation. Samples demonstrating spatially heterogeneous chemical features were evaluated post DESI-MS analysis and annotated by histopathologic review of frozen tissue sections. There were no cases in which histopathology review differed between frozen and formalin-fixed tissue sections. The annotated regions were used to define areas associated with non-malignant morphological features, unless otherwise noted.

Cytology

Following DESI-MS analysis, all FNA slides were stained with Wright's stain and evaluated by light microscopy. FNA slides were reviewed by an expert veterinary cytopathologist, who interpreted the nature of the sample (*i.e.* lymphoma vs. non-lymphoma), the distribution of cells within the sample (*i.e.* homogenous vs. heterogeneous distribution of cellular material within the smear), the density of cells within the sample (*i.e.* densely cellular vs. sparsely cellular), and whether significant red blood cell contamination of the sample was present.

Data Analysis

DESI-MS ion images

Surgical biopsy and FNA smear data acquired using XCalibur 2.0 (.raw) were converted with an in-house program into files compatible with BioMap software (http://www.maldi-msi.org). BioMap was used to generate 2D ion images (retaining spatial relationships and displaying relative mass spectral abundance of particular mass-to-charge ratios), select regions of interest (ROI) based on pathology, and export data for multivariate analysis. An in-house MatLab (MathWorks, Inc., Natick, MA, USA) routine was used to explore chemical features present in two dimensional DESI ion images. PCA was performed upon MS hyperspectral datacubes, the composite of spatial dimension ("x" and "y"), *m/z* value, and corresponding *m/z* intensity, and plotted using an interactive brushing procedure,[15] see Supplemental information for more details.

Multivariate analysis

PCA was used to explore DESI-MS data and visualize the grouping of samples resulting from chemical similarity.[16] Multivariate analysis of tissue sections was performed using in-house MatLab routines. The mass range was truncated (*m/z* 700-1000) for statistics, as it was empirically found to contain less analytical variability, providing more consistent and clear separation with regards to disease state (*i.e.* normal vs. tumor). Two specimens were excluded from statistics: one lymphoma sample (due to poor MS signal) and a metastatic carcinoma. MS data were normalized by the total ion current (TIC) and column-centered (*i.e.* mean-centered). Neither background subtraction nor a smoothing algorithm was applied to the MS data before PCA. LDA was performed for discriminant classification after unsupervised data compression by PCA (*i.e.* PCA-LDA), as reported elsewhere.[28] The first 8 principal components (PCs), accounting for ~90% of total data variation, were used. Classification rates report the correct classification of samples in the final PCA-LDA model. Cross validation (CV) with 5 deletion groups was used to test the prediction ability, reported as CV sensitivity and specificity. Sensitivity was calculated as the percent of the objects in the evaluation sets correctly accepted by the model. Specificity was calculated as the percent of the objects of other categories correctly rejected by the model. Average DESI mass spectra obtained from FNA smears were compared with those of surgical biopsy via multivariate statistics. A linear discriminant model (*i.e.* PCA-LDA) was built in PARVUS (University of Genova, Italy) using mass spectra from surgical biopsy tissue sections, to which FNA smear mass spectra were classified. The results and prediction rates are tabulated.

Results and Discussion

DESI-MS Imaging of Lymph Node Tissue Sections

Surgically excised lymph node biopsies were sectioned and analyzed by DESI-MS imaging, providing chemical and spatial information concurrently. The methodology employed follows that of histopathological evaluation of tissue, while providing molecular information. Tissue diagnosis by DESI-MS is performed with a spatial resolution larger than traditional histopathology (hundreds of microns versus tens of microns); however, it provides chemical information otherwise unobtainable by traditional histopathology. DESI-MS analysis of tissue sections aims to explore and establish the lipid profiles indicative of normal and NHL tumor subtypes. Negative mode DESI mass spectra showed ionized fatty acids

Analyst Accepted Manuscript

Please do not adjust margins

(*e.g.* oleic acid, *m/z* 281), fatty acid dimers, and glycerophospholipids from *m/z* 700 - 1000 (*e.g.* PI(38:4), *m/z* 885), **Supplemental Figure 1 and Supplemental Table 2**. The major glycerophospholipids (GPL) ions observed included major structural and signaling lipid classes: phosphatidylinositols (PI), phosphatidylserines (PS), phosphatidylethanolamines (PE), and phosphatidylglycerols (PG). The majority of lymphoma-containing tissue sections displayed a conserved pattern of lipids (*i.e.* ion, *m/z*, and corresponding relative abundance), or lipid profile, that contrasted markedly with that of normal tissue, and varied more slightly between B-cell and T-cell subtypes. Minute analytical variances in the lipid profile and signal intensity were attributed to freezing and sectioning artifacts. These small areas contributed insignificantly upon averaging and did not compromise the ability to ascertain MS information.

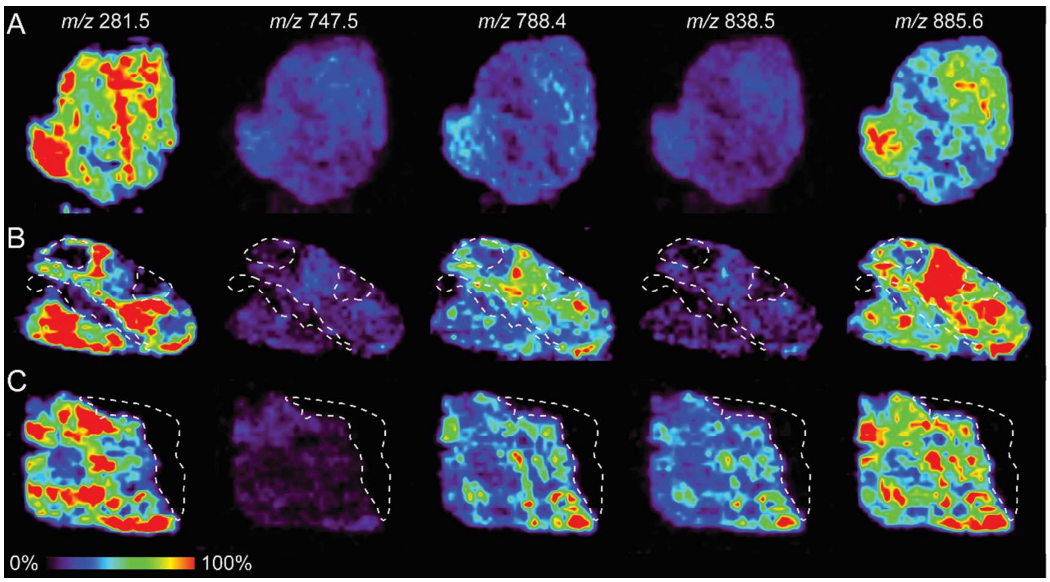

Fig 1. Selected negative mode DESI-MS ion images displaying the distribution of ions *m/z* 281.5, 747.5, 788.4, 838.5, and 885.6 and the corresponding H&E stain. (A) Specimen 18 is representative of B-cell lymphoma samples in regards to chemical and spatial homogeneity. (B) Specimen 31, B-cell lymphoma, contained small regions of perinodal adipose (outlined). (C) Specimen 42, illustrative of normal samples. The large region of perinodal adipose (outlined) was chemically difference than that of normal lymph node tissue.

DESI-MS ion images, two dimensional spatial distribution of *m/z* versus the corresponding ion abundance represented in false-color, revealed the majority of samples to be chemically homogenous, *i.e.* to have similar lipid profiles. Diffuse large B-cell lymphoma, Figure 1A was particularly homogenous, spatially and chemically, following the propensity of this cancer to diffusely obliterate normal lymph node architecture. Normal samples were also relatively homogenous in regards to chemical composition and spatial distribution. Interestingly, regions of normal lymph node anatomy, *e.g.* cortex and medulla, yielded nearly identical lipid profiles although differing in absolute MS intensity. The similarity of the lipid profile was unexpected as anatomical distribution of B-cell and T-cell lymphocytes is known to differ in lymph nodes: B-cells are found in densely packed follicles within the cortex and T-cells are present in the surrounding paracortex. The medulla contains a mixture of plasma cells, macrophages, and T-cells. The absolute MS signal intensity varied between the cortex and medulla, the latter yielded less signal. This intensity difference might result from the anatomical differences between the two regions that are not detected, such as the greater density of blood vessels and vascular sinuses within the lymph node medulla, which reduces the overall cellular density. The spatial resolution of DESI-MS data acquisition used does not allow for such anatomical structures to be visualized. MS imaging at higher resolution (<200 µm), possible by secondary-ion MS, matrix-assisted laser desorption, DESI, and nanoDESI,[12-14, 17] could visualize these anatomical regions with a non-linear increase in analysis time (analysis time increases with the reciprocal of the square of spatial resolution); however, investigation of normal lymph node anatomy is beyond the scope of the intended application.

Differences in the chemical information within analyzed tissue sections, disregarding previously discussed MS intensity differences, were noted in some of the normal and tumor specimens. In all of these instances (independent of tissue disease state, *i.e.* normal versus tumor) the difference resulted from the presence of perinodal adipose tissue, as determined by *post hoc* histopathology. Specimen 31 is illustrative, **Figure 1B**, a tissue section comprised primarily of a B-cell tumor with smaller regions of non-neoplastic, perinodal adipose tissue. The tumor regions have a common lipid profile that is homogenous throughout the tumor region; however, the lipid profile of small regions corresponding to perinodal adipose tissue (outlined) are significantly different and overall lower in absolute intensity as seen in the ion images (particularly *m/z* 281.5). The chemical difference of this region was further explored using PCA and an interactive brushing procedure, see **Supplemental Figure 2**. The PCA score plot, displaying each pixel of specimen 31, indicated three groups: B-cell lymphoma associated pixels (red selection), perinodal adipose associated pixels (green selection), and background associated pixels

Analyst Accepted Manuscript

This journal is © The Royal Society of Chemistry 20xx

(black). The results of visual interpretation and PCA correlated well with the pathological assessment, considering the differences in spatial resolution of MS imaging and histopathology. Perinodal adipose tissue was also detected in some normal lymph nodes, for example specimen 42, as shown in **Figure 1C**. The difference in the lipid profile was again evident between the two tissue types with negative mode GPL signal only noted in the lymph node parenchyma. The lack of GPL signal in adipose tissue is likely correlated to adipocytes (*i.e.* fat cells), which typically possess a large cytoplasmic volume to GPL membrane surface area ratio. Further, adipocytes contain greater levels of triglycerides and cholesteryl esters which are not readily detected in the negative mode with the solvent conditions chosen; however, previous DESI experiments have detected such compounds in positive ion mode from biological material with relative ease as silver adducts.[30]

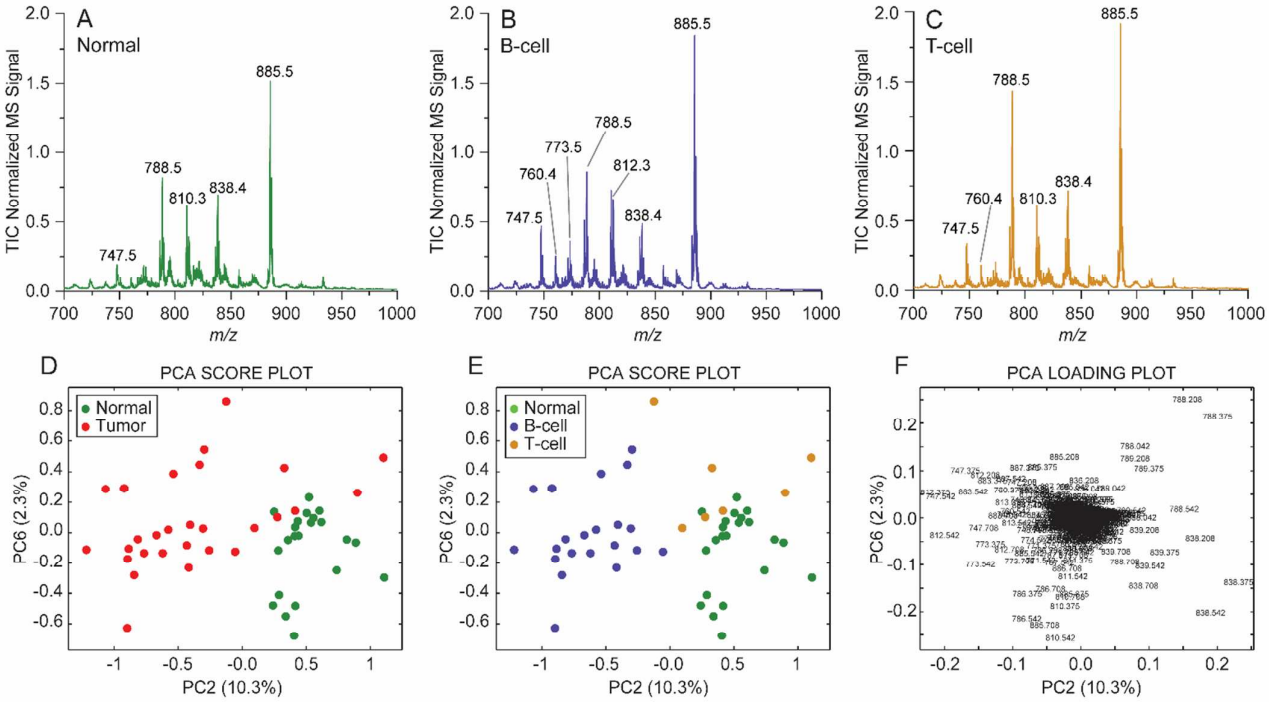

Fig 2. Average negative mode DESI mass spectrum of tissue sections: (A) normal lymph node (n=22), (B) B-cell lymphoma (n=22), and (C) T-cell lymphoma (n=7). (D) PCA score plot of normal (green) and tumor (red) samples. (E) PCA score plot of normal (green), B-cell lymphoma (blue), and T-cell lymphoma (gold) samples. (F) PCA loading plot corresponding to panel D&E with *m/z* annotated.

Differentiating Lipid Profiles in NHL Tissue Sections

The lipid profiles of tissue sections were explored for molecular-based differentiation of disease state (normal versus tumor) and NHL tumor subtype (*i.e.* B-cell versus T-cell). The average DESI mass spectrum (from *m/z* 700 - 1000) of normal lymph node (n=22), B-cell lymphoma (n=22), and T-cell lymphoma (n=7) tissue sections, green, blue, and gold respectively, are displayed in **Figure 2A-C**. The ratio of MS abundance of *m/z* 788.3, 838.3, and 885.5 indicated, visually, molecular differences between disease states. Nearly all B-cell samples were diagnosed as diffuse large B-cell lymphoma, differences in the lipid profile are noted in comparison to the average normal spectrum. A small number of T-cell lymphoma tissue sections were analyzed, diagnosed as peripheral T-cell lymphoma, not otherwise specified (n=4) and T-zone lymphoma (n=3). Spectral differences were also noted between normal and T-cell NHL, but the limited number of samples and multiple T-cell subtypes preclude definitive conclusions. Less abundant peaks present in B-cell and T-cell lymphoma also differed in abundance from normal samples including *m/z* 747.4, 773.3, 786.4, 812.4, 883.5. These ions and their altered relative abundance mirror those reported previously by Eberlin et al. in murine and human lymphoma specimens.[31] One metastatic carcinoma, specimen 12, was analyzed and yielded different lipid profiles from normal and lymphoma with strong alterations in *m/z* 819, 834, 865, and 867 (**Supplemental Figure 3**). Abbassi-Ghadi and coworkers have previously analyzed metastatic tumors in lymph nodes by DESI, concluding that the chemical information corresponded to that of the primary tumor and had clearly different from adjacent normal lymph node.[32] Extrapolating from that work, the lipid profile of specimen 12 might correlate with that of the primary tumor; however, biopsies of the primary tumor were not available for analysis.

Principal component analysis was performed on the average spectrum of each tissue section, offering an unbiased method for qualitatively assessing the molecular information associated with the pathology-defined condition. Disease state differentiation (normal vs. tumor) was the initial level of diagnostic information explored. Normal lymph node (green) and tumor (red) samples were appropriately grouped as shown in **Figure 2D**. Dispersion of the tumor samples in the

Analyst Accepted Manuscript

PCA score plot, compared with the normal samples, is indicative of greater chemical heterogeneity within lymphoma – matching known diversity of the disease.[1] The dispersion of the lymphoma samples appears to be related to tumor immunophenotype, **Figure 2E**: normal (green), B-cell lymphoma (blue), and T-cell lymphoma (gold). The PCA loading plot, displayed in **Figure 2F**, aided in understanding which lipids from *m/z* 700 - 1000 contributed most to PC2 and PC6 computations (see **Supplemental Figure 4** for additional information). Distinguishing NHL subtypes represents a deeper level of diagnostic information, which commonly requires IHC/ICC; the chemical information obtained by DESI may circumvent or augment such protocols. The separation of B-cell and T-cell lymphoma is suggested in **Figure 2E**; however, expansion of NHL subtypes is necessary to confirm this initial report. More detailed exploration of the chemical differences was performed by iterative study of the relationship between disease states rather than together as in **Figure 2.** For example, the chemical difference between B-cell and T-cell NHL tumors is more apparent upon removal of normal samples (**Supplemental Figure 5**). The separation noted must be taken as preliminary, particularly for T-cell tumors, based on the relatively small sample size and known genetic diversity of lymphomas. The ability to subtype tumors using DESI-MS has been previously demonstrated, *e.g.* brain and kidney tumors,[13, 18] but has not been previously reported in lymphoma. Diagnostic information acquired by DESI would serve to support pathological diagnosis, particularly relating to tumor subtyping as an alternative to IHC.

The discriminatory performance of DESI-MS in determining disease state and subsequently tumor subtype from tissue sections was explored via PCA-LDA. The classification rate in PCA-LDA model creation was 100% for normal and tumor. Cross-validation was performed resulting in the predicted sensitivity and specificity results displayed in **Table 1**. Further, PCA-LDA was performed separately taking the lymphoma subtypes into consideration, modelling classification rates were 100%, 99% and 94 % for normal, B-cell, and T-cell respectively. CV indicated two misclassifications (T-cell predicted as normal, and B-cell predicted as T-cell). The predicted sensitivity and specificity for NHL subtyping is tabulated in **Table 2.** The CV sensitivity of T-cell lymphoma (85.7%) was relatively poor in comparison to the other states (normal, 100% and B-cell lymphoma, 95.5%), likely the result of a smaller sample size (n=7) or the presence of two different subtypes (*i.e.* peripheral and T-zone).

Table 1. CV results of DESI-MS in discriminating disease state (normal vs. tumor) in tissue sections

		Pathological Diagnosis	
		Normal	Tumor (B- & T-cell NHL)
DESI-MS Prediction	Normal	22	2
	Tumor (B- & T-cell NHL)	0	27
CV Sensitivity (%)		100.0	93.1
CV Specificity (%)		93.1	100

Table 2. CV results for NHL subtyping of tissue sections by DESI-MS

		Pathological Diagnosis		
		Normal	B-cell NHL	T-cell NHL
DESI-MS Prediction	Normal	22	0	1
	B-cell NHL	0	21	0
	T-cell NHL	0	1	6
CV Sensitivity (%)		100	95.5	85.7
CV Specificity (%)		96.4	100	97.7

DESI-MS Imaging of Fine Needle Aspirates

Histopathological evaluation of surgically excised lymph nodes, the gold standard for lymphoma diagnosis, is an invasive procedure and therefore not suitable for rapid preliminary diagnosis of NHL. Fine needle aspirate biopsy is a less expensive, less invasive, and less technically demanding method, and therefore a reasonable alternative. FNA tend to be less reliable than surgical biopsy, in part due to the limited discriminatory ability of cytology in comparison to histopathology. However, DESI-MS analysis of FNA smears provided molecular information that is similar to that of tissue sections and offers an alternative to FNA cytology, aimed at enhancing diagnostic capability.

FNA smears, prepared using standard protocols, were analyzed without any pre-treatment. DESI-MS was performed on a small area of the smear, not the entirety of the smear, representing a time reducing strategy for preliminary diagnosis. It was assumed that aspiration and subsequent smearing, was sufficiently homogenizing. The MS data obtained from FNA smears were highly reminiscent of those for surgical biopsy tissue sections. The average mass spectra for normal and B-cell lymphoma are displayed in **Figure 3**, with more detail provided in **Supplemental Figure 6**. The chemical information obtained from FNA appears to be identical in nature to that of tissue sections suggesting that the type of sample does not impact ability to acquire chemical information correlated to disease state. The strategy of using DESI spectra obtained from tissue sections serves as an important reference in this case, having been used previously in cancer diagnosis,[11, 13, 18, 19] thus allowing evaluation of FNA as a new type of sample for the same DESI methodology.

Analyst Accepted Manuscript

This journal is © The Royal Society of Chemistry 20xx

Please do not adjust margins

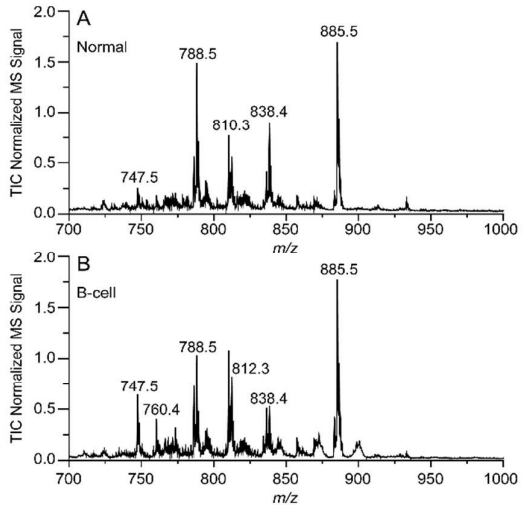

Fig 3. Average (-)DESI-MS spectrum for (A) normal FNA (n=7) and (B) B-cell lymphoma FNA (n=28).

Unsurprisingly, subtle differences do exist between tissue sections and FNA smears which did not preclude acquisition of mass spectral information but rather influenced data quality. FNA smears were nearly always chemically homogenous, *i.e.* the lipid profile was similar in all areas of the smear, supporting the assumption of sufficient homogenization, while difference in the signal intensity were common (**Supplemental Figure 7**). Two major variables in FNA smears were found to affect MS intensity: the quantity of cellular material aspirated and the degree of dilution due to smearing. The effect of quantity is noted in **Supplemental Figure 8** in which the heterogeneity present in the ion image results from variable amount of material – signal intensity is correlated with material quantity. The second variable is the degree of smearing of the aspirated sample which dilutes the cellular material on the glass slide. This dilution is necessary for cytologic evaluation using light microscopy, in which morphologic evaluation of isolated cells is desirable, but is deleterious for chemical analysis by DESI-MS. Slight modification to current FNA protocols that compensate for these effects is likely to increase DESI reproducibility, MS data quality, and capability for molecular diagnosis. Additionally, differences in the lipid profile were noted in cases of obvious blood contamination of the aspirated sample, resulting in a visually red coloration to the smear. The presence of blood contamination significantly increased one particular lipid, *m/z* 810, which corresponds to PS(40:6), a major membrane constituent of erythrocytes[33] and therefore easily detected. Minor blood contamination did not seem to compromise the ability to determine disease state. Subsequent staining of FNA smears (Wright's stain) analyzed by DESI and evaluation by light microscopy, indicated cellular damage, which could result from physical damage during smearing or freeze thaw cycle. Certainly, DESI has the potential to produce the observed cellular damage via physical (*e.g.* pneumatic) forces or chemical fixation (*i.e.* organic solvent). An expert cytopathologist commented that the morphologic changes in the cells appeared similar to those commonly observed in samples exposed to formalin, a common chemical fixative, which supports the latter reason for the observed effect. This observation is quite interesting in that it contrasts the preservation of morphology during analysis of histologic tissue sections – no effect on histomorphology is noted using dimethylformamide-acetonitrile as a DESI solvent system. One biological reason for this observation is the presence of stromal tissue and extracellular matrix in histologic sections, which may minimize the cellular damage of DESI analysis relative to what was observed in FNA smears, which would presumably contain less of these protective elements.

Differentiation of Disease State using FNA Smears

The chemical information obtained using DESI-MS from FNA smears was evaluated by multivariate statistics, undertaken to determine FNA's potential diagnostic performance and explore how translatable the chemical information obtained from tissue sections are to FNA smears. In clinical practice, the information relevant in FNA evaluation is the presence or absence of tumor, and serves only to provide a rapid, preliminary diagnosis which requires subsequent confirmation by more accurate methods such as histopathology. PCA-LDA was applied and performed by building a classification training set using tissue section data and evaluating the FNA smear data. PCA-LDA prediction rates are displayed in **Table 3.** Prediction of normal was 85.7% and tumor was 89.3%. The preliminary results displayed indicate that DESI-MS analysis of FNA smears has diagnostic potential. Further, the results support that the chemical information relevant to disease state is equivalently detected by DESI-MS. FNA smears, neither adapted nor optimized for MS analysis, provided reasonable classification results, provided that FNA smears are known to be less reliable than surgical biopsy samples evaluated by histopathology.

Table 3. PCA-LDA prediction of FNA smears analyzed by DESI-MS

		Pathological Diagnosis	
		Normal	B-cell NHL
DESI-MS Prediction	Normal	6	3
	B-cell NHL	1	25
PCA-LDA Prediction Rate		85.7%	89.3%

*Note four ROIs were taken for specimen 8, 13, and 19, and two ROIs from specimen 35

Beyond the rapid molecular diagnosis of NHL by DESI-MS via FNA analysis, the envisioned application, has the potential for rapid tumor subtyping. PCA cross-validation of tissue sections indicated the possibility for tumor subtyping; however, this could not be explored based on FNA sample numbers. Surely, this requires a larger and more diverse sample set, particularly with knowledge of NHL tumor heterogeneity. The primary goal of FNA analysis by DESI was demonstrated: rapid molecular-based dichotomous delineation of disease state (*i.e.* normal and tumor), which has

Analyst Accepted Manuscript

Please do not adjust margins

potential to be a significant advancement in the rapid diagnosis of non-Hodgkin's lymphoma.

Conclusion

Differences in the lipid profile, acquired by DESI-MS, allowed differentiation of normal lymph node and NHL tumors in tissue sections (obtained by surgical biopsy) and FNA smears. DESI-MS imaging of tissue sections allowed chemical information to be obtained and explored. Normal lymph node tissue was chemically homogenous while differences in absolute signal were noted between regions of normal lymph node anatomy, *e.g.* medulla and cortex. Tumor samples were generally homogenous, particularly diffuse large B-cell lymphoma samples, matching known histomorphology. Multivariate statistics allowed for differentiation of normal and tumor tissue sections yielding an overall predicted CV sensitivity of 96%. Further, subtyping of NHL tumors is suggested with an equal rate of predicted classification.

FNA smears, previously unexplored for use in diagnosis using ambient ionization – mass spectrometry, provided the same chemical information relevant to disease state differentiation detected from tissue sections. FNA smear data applied to a tissue section-based classification system yielded an average prediction rate of 87.5% for disease states. MS signal was dependent on the composition (*e.g.* blood contamination), aspirated material quantity and smearing. The act of smearing of FNA, while ideal for cytology, dilutes the cellular material necessary for DESI-MS lipid analysis. Improvement in the protocols for FNA preparation, with tailoring specifically for MS analysis is likely to improve results. The molecular information detected from FNA smears are not subject to the same set of problems (*e.g.* physical damage of cells) experienced in cytopathology, and therefore could improve diagnostic yield. Cellular damage was noted after DESI analysis upon FNA samples, effecting only subsequent pathology and not the molecular information. The reason for this damage is presently unknown, but might result from chemical damage. Analysis of FNA material by other ambient methods such as PESI or paper spray ionization represents another possible direction of development.[34] The direct aspiration of material onto paper for PS analysis eliminates smearing and may provide additional advantages in regards to MS analysis. The informative but less invasive collection of FNA smears, also performed during diagnosis of other cancers, particularly those of the breast, thyroid, and salivary gland, is clearly best suited to answer the question of rapid preliminary diagnosis, "Is this sample normal or cancerous?"

DESI-MS analysis of tissue sections provided a means of exploring and establishing the lipid profiles indicative of normal lymph node and NHL tumors. FNA smears mimic those changes, primarily in GPL composition, which are certainly related to cellular and morphological changes that occur with NHL. The polar lipids detected in the negative ion mode represent only a fraction of metabolites, and further study of the metabolome may reveal additional diagnostic information. The subtype prevalence, clinical behavior, and chemical changes in GPL emulate that of human NHL,[20] supporting development of canine comparative models. The methodology outlined here is applicable to dogs while translation to humans is foreseeable.

Acknowledgements

The authors thank Dr. Christina Ferreira and Dr. Paolo Oliveri for their contributions. Funding support was provided by Purdue University Center for Cancer Research SIRG Program, Award 8000062024.

References

1 D. Ito, A. M. Frantz and J. F. Modiano, *Veterinary Immunology and Immunopathology*, 2014, **159,** 192-201.
2 NIH-NCI, SEER Stat Fact Sheets: Non-Hodgkin Lymphoma, 2014.
3 L. Marconato, M. E. Gelain and S. Comazzi, *Hematological Oncology*, 2013, **31,** 1-9.
4 V. E. Valli, M. San Myint, A. Barthel, D. Bienzle, J. Caswell, F. Colbatzky, A. Durham, E. Ehrhart, Y. Johnson and C. Jones, *Veterinary Pathology*, 2011, **48,** 198-211.
5 F. Ponce, T. Marchal, J. Magnol, V. Turinelli, D. Ledieu, C. Bonnefont, M. Pastor, M. Delignette and C. Fournel-Fleury, *Veterinary Pathology*, 2010, **47,** 414-433.
6 S. T. Hehn, T. M. Grogan and T. P. Miller, *Journal of Clinical Oncology*, 2004, **22,** 3046-3052.
7 D. K. Das, *Diagnostic Cytopathology*, 1999, **21,** 240-249.
8 O. Landgren, A. Porwit MacDonald, E. Tani, M. Czader, G. Grimfors, L. Skoog, A. Ost, C. Wedelin, U. Axdorph and E. Svedmyr, *The Hematology Journal*, 2004, **5,** 69-76.
9 A. Venter, P. E. Sojka and R. G. Cooks, *Analytical Chemistry*, 2006, **78,** 8549-8555.
10 A. B. Costa and R. Graham Cooks, *Chemical Physics Letters*, 2008, **464,** 1-8.
11 J. Oetjen, K. Veselkov, J. Watrous, J. S. McKenzie, M. Becker, L. Hauberg-Lotte, J. H. Kobarg, N. Strittmatter, A. K. Mróz, F. Hoffmann, D. Trede, A. Palmer, S. Schiffler, K. Steinhorst, M. Aichler, R. Goldin, O. Guntinas-Lichius, F. von Eggeling, H. Thiele, K. Maedler, A. Walch, P. Maass, P. C. Dorrestein, Z. Takats and T. Alexandrov, *Gigascience*, 2015, **4,** 20.
12 R. D. Addie, B. Balluff, J. V. Bovée, H. Morreau and L. A. McDonnell, *Analytical Chemistry*, 2015, **87,** 6426-6433.
13 A. Bodzon-Kulakowska and P. Suder, *Mass Spectrometry Reviews*, 2015, doi: 10.1002/mas.21468.
14 C. Wu, A. L. Dill, L. S. Eberlin, R. G. Cooks and D. R. Ifa, *Mass Spectrometry Reviews*, 2013, **32,** 218-243.
15 X. Xiong, W. Xu, L. S. Eberlin, J. M. Wiseman, X. Fang, Y. Jiang, Z. Huang, Y. Zhang, R. G. Cooks and Z. Ouyang, *Journal of American Society for Mass Spectrometry*, 2012, **23,** 1147-1156.
16 J. C. Vickerman, *Analyst*, 2011, **136,** 2199-2217.
17 A. L. Dill, D. R. Ifa, N. E. Manicke, A. B. Costa, J. A. Ramos-Vara, D. W. Knapp and R. G. Cooks, *Analytical Chemistry*, 2009, **81,** 8758-8764.

Analyst Accepted Manuscript

This journal is © The Royal Society of Chemistry 20xx

Please do not adjust margins

18 J. M. Wiseman, S. M. Puolitaival, Z. Takáts, R. G. Cooks and R. M. Caprioli, *Angewandte Chemie*, 2005, **117,** 7256-7259.
19 L. S. Eberlin, I. Norton, D. Orringer, I. F. Dunn, X. Liu, J. L. Ide, A. K. Jarmusch, K. L. Ligon, F. A. Jolesz and A. J. Golby, *Proceedings of the National Academy of Sciences*, 2013, **110,** 1611-1616.
20 A. L. Dill, L. S. Eberlin, C. Zheng, A. B. Costa, D. R. Ifa, L. Cheng, T. A. Masterson, M. O. Koch, O. Vitek and R. G. Cooks, *Analytical and Bioanalytical Chemistry*, 2010, **398,** 2969-2978.
21 K. S. Kerian, A. K. Jarmusch, V. Pirro, M. Koch, T. Masterson, L. Cheng and R. G. Cooks, *Analyst*, 2015, **140,** 1090-1098.
22 L. S. Eberlin, R. J. Tibshirani, J. Zhang, T. A. Longacre, G. J. Berry, D. B. Bingham, J. A. Norton, R. N. Zare and G. A. Poultsides, *Proceedings of the National Academy of Sciences*, 2014, **111,** 2436-2441.
23 S. Santagata, L. S. Eberlin, I. Norton, D. Calligaris, D. R. Feldman, J. L. Ide, X. Liu, J. S. Wiley, M. L. Vestal and S. H. Ramkissoon, *Proceedings of the National Academy of Sciences*, 2014, **111,** 11121-11126.
24 J. Liu, R. G. Cooks and Z. Ouyang, *Analytical Chemistry*, 2011, **83,** 9221-9225.
25 L. S. Eberlin, C. R. Ferreira, A. L. Dill, D. R. Ifa, L. Cheng and R. G. Cooks, *ChemBioChem*, 2011, **12,** 2129-2132.
26 V. Pirro, L. S. Eberlin, P. Oliveri and R. G. Cooks, *Analyst*, 2012, **137,** 2374-2380.
27 R. Bro and A. K. Smilde, *Analytical Methods*, 2014, **6,** 2812-2831.
28 C. R. Ferreira, V. Pirro, L. S. Eberlin, J. E. Hallett and R. G. Cooks, *Analytical and Bioanalytical Chemistry*, 2012, **404,** Electronic Supplementary Material.
29 J. Laskin, B. S. Heath, P. J. Roach, L. Cazares and O. J. Semmes, *Analytical Chemistry*, 2011, **84,** 141-148.
30 V. Pirro, P. Oliveri, C. R. Ferreira, A. F. González-Serrano, Z. Machaty and R. G. Cooks, *Analytica Chimica Acta*, 2014, **848,** 51-60.
31 L. S. Eberlin, M. Gabay, A. C. Fan, A. M. Gouw, R. J. Tibshirani, D. W. Felsher and R. N. Zare, *Proceedings of the National Academy of Sciences*, 2014, **111,** 10450-10455.
32 N. Abbassi-Ghadi, K. Veselkov, S. Kumar, J. Huang, E. Jones, N. Strittmatter, H. Kudo, R. Goldin, Z. Takáts and G. Hanna, *Chemical Communications*, 2014, **50,** 3661-3664.
33 K. Leidl, G. Liebisch, D. Richter and G. Schmitz, *Biochimica et Biophysica Acta (BBA)-Molecular and Cell Biology of Lipids*, 2008, **1781,** 655-664.
34 C. H. Lin, W. C. Liao, H. K. Chen and T. Y. Kuo, *Bioanalysis*, 2014, **6,** 199-208.

Analyst Accepted Manuscript

Please do not adjust margins